

Systematic Monte-Carlo studies of dijets at RHIC using the VNI/BMS Parton Cascade

C.E.Coleman-Smith

E-mail: cec24@phy.duke.edu

Department of Physics, Duke University, Durham, NC 27701

Abstract. We present a study of the dijet suppression at RHIC using the parton cascade model. We examine the modification of the dijet asymmetry A_j and the fragmentation distributions z and j_T in terms of: \hat{q} ; the path length of leading and sub-leading jets; cuts on the jet energy distributions; jet cone angle and the jet-medium interaction mechanism. We have introduced a string hadronization model and present hadronic jet fragmentation distributions. We find that A_j is most sensitive to \hat{q} and less sensitive to the nature of the jet-medium interaction mechanism. The fragmentation distributions show jet modification and differentiate between elastic and radiative+elastic modes.

Measurements showing the modification of high energy $E_t \sim 100\text{--}200$ GeV dijets at the Large Hadron Collider (LHC) [1, 2] in Pb+Pb collisions have sparked an interest in using dijets to quantify jet modification in hot QCD matter. Proposed upgrades to the PHENIX experiment, and the continuing development of jet measurements at STAR promise access to dijets with $E_t \sim 15\text{--}65$ GeV at RHIC. The dijet asymmetry

$$A_j = \frac{E_{t,\ell} - E_{t,s}}{E_{t,\ell} + E_{t,s}}, \quad (1)$$

where $E_{t,\ell}$ is the transverse energy of the leading jet and $E_{t,s}$ is that of the sub-leading jet, has been successfully reproduced with a variety of models [3, 4, 5, 6, 7]. It is not obvious that the dijet asymmetry is the most suitable quantity for measuring the modification of dijets. Given that the dijet program at RHIC is still in its infancy it is worthwhile to consider the existence of other perhaps more differential observables.

We have used the VNI/BMS [8, 9] parton cascade to systematically explore dijet suppression at RHIC energy scales under controlled medium conditions. We examine the modification of dijets under variation of the medium radius and temperature, the strong coupling constant and the jet definition in terms of the Anti-Kt cone angle and the leading jet energy cut. The VNI/BMS parton cascade model provides access to the full jet/medium development at a fixed temperature and density, and thus fixed \hat{q} . We run the code in a static uniform-medium mode.

The full set of results from our systematic analysis can be found in [10]. In this proceeding we outline the model, introduce the hadronization process and show some selected results from the analysis.

The parton cascade model (PCM) is a Monte-Carlo implementation of the relativistic

Boltzmann transport of quarks and gluons

$$p^\mu \frac{\partial}{\partial x^\mu} F_k(x, p) = \sum_i \mathcal{C}_i F_k(x, p). \quad (2)$$

The collision term \mathcal{C}_i includes all possible $2 \rightarrow 2$ interactions and final-state radiation $1 \rightarrow n$

$$\mathcal{C}_i F_k(x, \vec{p}) = \frac{(2\pi)^4}{2S_i} \int \prod_j d\Gamma_j |\mathcal{M}_i|^2 \delta^4(P_{in} - P_{out}) D(F_k(x, \vec{p})), \quad (3)$$

$d\Gamma_j$ is the Lorentz invariant phase space for the process j , D is the collision flux factor and S_i is a process dependent normalization factor. A geometric interpretation of the total cross-section is used to select pairs of partons for interaction. Between collisions, the partons propagate along straight line trajectories.

In the VNI/BMS PCM outgoing (from a hard scattering) off-shell partons are brought back on-shell through a medium modified time-like branching, this includes a Monte-Carlo Landau-Pomeranchuk-Migdal (LPM) effect [11, 5, 12, 13]. The radiated partons are assigned a formation time which is dynamically modified by further elastic interactions which generally serve to reduce the initial formation time. The shower partons are unable to radiate until their formation time has expired. This naturally builds a spatial dependence into the radiation process.

The strong coupling constant is fixed at $\alpha_s = 0.3$. A QGP medium is simulated as a box of thermal quarks and gluons generated at some fixed temperature. Periodic boundary conditions are imposed on the box, whose size is selected to be large enough that if a simulated jet wraps around it will not interact with its own wake.

The partonic contents of jets created by a suitable event generator and evolved down to $Q_0 = 1$ GeV, in this study PYTHIA 8 [14], are directly inserted into the box of thermal quarks and gluons. Each jet from the dijet pair is evolved separately. The jet partons propagate for a given distance and their evolution is recorded. Each particle in the initially inserted jet is marked as being ‘‘jetty’’, this jettiness tag is then iteratively applied to all partons that interact with an already jetty-labeled parton.

We have developed a simple scheme for hadronizing the contents of these jets which follows the Les Houches accord for particle color labeling. We extract the colors labels of the initial partons from the event generator. As these partons interact over the evolution of the jet the color labels are propagated appropriately. Each medium parton is given the next free color label. The partons interact through color averaged cross-sections. After including contributions from the medium the jet is in usually a non singlet state. We neutralize this color structure by generating a minimal set of thermal partons with appropriate color labels to reduce the jet to a color singlet state. The final set of partons is hadronized through the Lund string model [15].

In Fig. 1 we show a comparison of the partonic and hadronic transverse and longitudinal momentum distributions for a 100 GeV quark jet evolved in a box at $T = 0.35$ GeV for 4 fm/c. The dashed blue curve shows the distributions of the jet partons along with the associated thermal color-matching partons, these additional partons lead to an enhancement at small P_T and small z . Hadronization smooths and softens the longitudinal momentum distribution, conservation of momentum leads to an associated constriction of the transverse distribution.

We consider dijets at RHIC scales $\sqrt{s_{NN}} = 200$ GeV, all jets are reconstructed with the Anti-Kt algorithm [16]. The following kinematic cuts were always imposed: the minimum jet cut is set to $p_{t,min} = 5$ GeV, $\Delta|\eta_{12}| < 1.1$, $\Delta\phi_{12} > \pi/2$ where $\Delta\eta_{12}$ and $\Delta\phi_{12}$ are measured between the two reconstructed jets in the event. In this kinematic region the mean jet $\langle Et \rangle \sim 30$ GeV.

In Fig. 2 we show the influence of varying the medium temperature on the dijet asymmetry A_j . Recall that perturbative calculations for \hat{q} scale like T^3 . The higher temperature $T = 0.35$ GeV

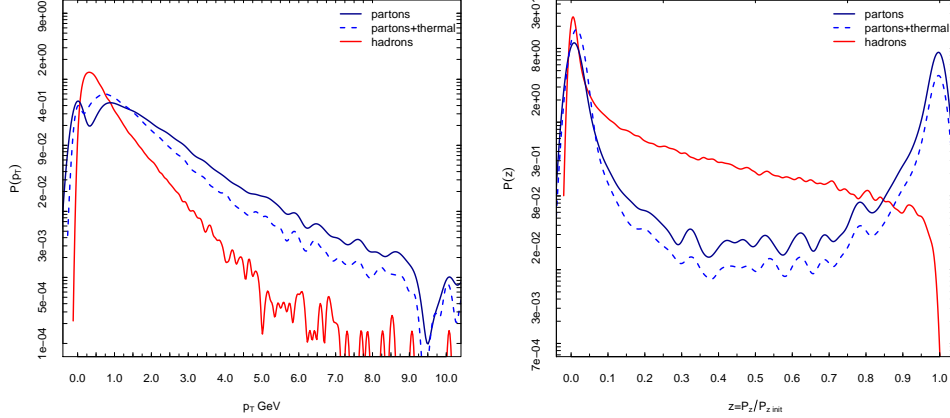


Figure 1. (Color Online) Transverse (left) and longitudinal (right) momentum distributions for the contents of 100 GeV quark jet evolved in a box at $T = 0.35$ GeV for 4 fm. Partonic distributions are shown as the blue curves, hadronic curves in red. The dashed blue curve represents the partonic distributions after the addition of the thermal partons required for hadronization

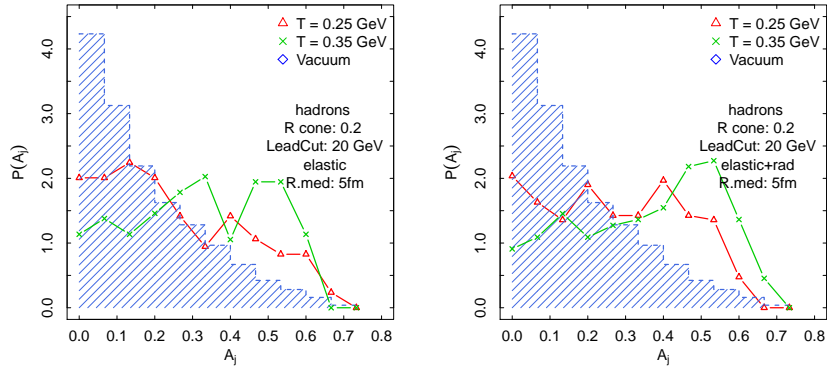


Figure 2. (Color Online) Elastic (left) and Elastic+Radiation (right) distributions of A_j as a function of the medium temperature, for hadrons. The shaded blue histogram shows the vacuum (PYTHIA) results.

(green curve, crosses) leads to a strong increase in the observed asymmetry for both interaction mechanisms. The full simulation (right panel), including elastic and radiative results, shows a somewhat stronger asymmetry than the elastic only result. This shift is observed to be strongest at small jet cone radii, here we have used $R = 0.2$. Increasing the cone radius “recaptures” the escaped energy and so tends to reduce the observed asymmetry, see Fig. 3 and [10].

We plot the longitudinal jet fragmentation $z = \frac{p_{t,h}}{p_{t,jet}} \cos \Delta r$ in Fig. 3, for leading (closed symbols) and sub-leading (open symbols) dijets. The plots show the vacuum distributions (blue, dashed) and the evolved distributions (red, solid). Let us first consider the left panel, which shows jets reconstructed at $R = 0.2$. There is a strong peak at $z = 1$. The limited phase space for the vacuum evolution of the jets at RHIC scales frequently gives rise to jets which have not undergone many splittings. The longitudinal momentum distribution for these jets is dominated by one or two very hard partons. This peak is diminished by evolution, with a concomitant enhancement at small z for the evolved jets. Since z is normalized to the final-state measured jet momentum, the medium induced energy loss is mostly scaled out.

The right hand panel of Fig. 3 shows the fragmentation distribution for the same events but calculated with a much wider jet cone angle $R = 1.0$. The peak at $z = 1$ is still just evident in the vacuum distributions. There is a clear separation between the evolved and vacuum distributions (blue,red). The small z peak is enhanced by medium induced radiation, forward scattering and the fragmentation process itself (as shown in Fig. 1). These two extremes paint a picture of jets as having a hard core surrounded by a more diffuse cone of soft partons from medium induced radiation and forward elastic scattering.

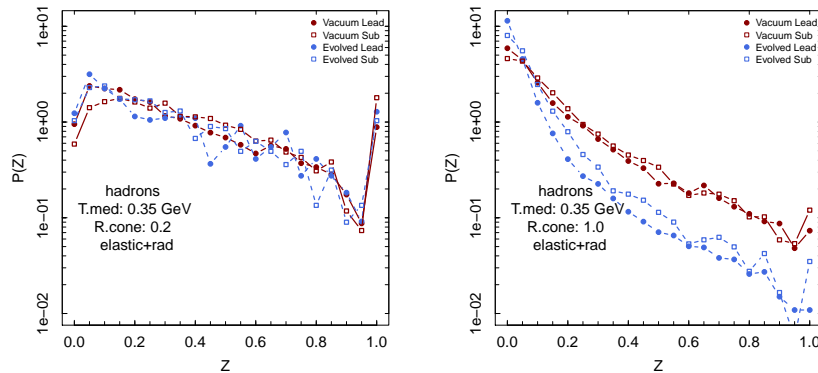


Figure 3. (Color Online) Longitudinal jet fragmentation z distributions for evolved (red, solid lines) and vacuum (blue, dashed lines) dijets reconstructed at $R = 0.2$ (left) and $R = 1.0$ (right). The (sub-leading, leading) dijet results are shown with (filled,open) symbols. Note that these curves are normalized to unit area.

Dijets at RHIC scales are likely to be strongly modified by the presence of the deconfined QGP medium. The observables we have discussed are sensitive to many aspects of this modification and suggest that further jet measurements at RHIC will provide valuable insights into the nature of the QGP.

We acknowledge support by DOE grants DE-FG02-05ER41367 and DE-SC0005396. This research was done using computing resources provided by OSG EngageVo funded by NSF award 075335.

References

- [1] Aad G *et al.* (Atlas) 2010 *Phys. Rev. Lett.* **105** 252303
- [2] Chatrchyan S *et al.* (CMS Collaboration) 2011 *Phys.Rev.* **C84** 024906
- [3] Qin G Y and Müller B 2011 *Phys. Rev. Lett.* **106** 162302
- [4] Young C, Schenke B, Jeon S and Gale C 2011 (*Preprint 1103.5769*)
- [5] Coleman-Smith C E, Bass S A and Srivastava D K 2011 (*Preprint 1101.4895*)
- [6] He Y, Vitev I and Zhang B W 2011 (*Preprint 1105.2566*)
- [7] Renk T 2012 (*Preprint 1202.4579*)
- [8] Geiger, Klaus and Müller, Berndt 1992 *Nucl. Phys.* **B369** 600–654
- [9] Bass S A, Müller B and Srivastava D K 2003 *Phys. Lett.* **B551** 277–283
- [10] Coleman-Smith C E and Muller B 2012 *Phys.Rev.* **C86** 054901 (*Preprint 1205.6781*)
- [11] Zapp K, Stachel J and Wiedemann U A 2009 *Phys. Rev. Lett.* **103** 152302
- [12] Landau L D and Pomeranchuk I J 1953 *Dolk. Akad. Nauk. SSSR* **92**
- [13] Migdal A B 1956 *Phys. Rev.* **103** 1811–1820
- [14] Sjöstrand T, Mrenna S and Skands P Z *JHEP* **0605** 026
- [15] Andersson B 1997 *Camb.Monogr.Part.Phys.Nucl.Phys.Cosmol.* **7** 1–471
- [16] Cacciari M, Salam G P and Soyez G 2008 *JHEP* **04** 063 (*Preprint 0802.1189*)